Optical helicity, chirality, and spin of 3D-structured Laguerre-Gaussian optical vortices

Forbes, Kayn, Jones, Garth

Kayn A. Forbes, Garth A Jones, "Optical helicity, chirality, and spin of 3D-structured Laguerre-Gaussian optical vortices," Proc. SPIE 12017, Complex Light and Optical Forces XVI, 1201708 (2 March 2022); doi: 10.1117/12.2605929

SPIE.

Event: SPIE OPTO, 2022, San Francisco, California, United States

Optical helicity, chirality, and spin of 3D-structured Laguerre-Gaussian optical vortices

Kayn A. Forbes* and Garth A. Jones

School of Chemistry, University of East Anglia, Norwich NR4 7TJ, United Kingdom

*k.forbes@uea.ac.uk

ABSTRACT

Optical fields possess energy, momentum, and helicity. For the plane waves and paraxial fields of standard, classical optics, the spin angular momentum and optical helicity are well understood, both being proportional to the degree of circular polarization. In contrast, 3D non-paraxial optical fields generated by spatial confinement, such as tight focusing and evanescent waves, may possess spin angular momentum and optical helicity when the degree of 2D-circular polarization is zero. In this work using quantum electrodynamics we highlight two novel properties of non-paraxial optical vortices 1) a non-zero optical helicity (chirality) density for 2D-unpolarized (and 2D-linearly polarized) 3D optical vortices and 2) a longitudinal spin angular momentum density for 2D-linearly polarized 3D optical vortices.

Keywords: Optical helicity, optical chirality, chirality, spin angular momentum, optical angular momentum nanophotonics, structured light, twisted light

1. INTRODUCTION

Electromagnetic fields possess a range of conserved dynamical properties[1], each of which manifest in distinct physical observables in experiments. Most important are the energy, linear momentum, spin angular momentum (SAM), orbital angular momentum (OAM), and optical helicity. For the most well-known optical fields, such as propagating plane waves and paraxial laser beams, the values of these conserved quantities in relation to the polarization and spatial degrees of freedom have long been well understood, being found throughout undergraduate textbooks on optics and electrodynamics[2–4]. However, with the advent of nanophotonics there was required a new approach, where the non-paraxial nature of spatially confined optical fields had to be addressed and exploited[5]. The novel physics and widespread applications of non-paraxial fields in nanophotonics is breath-taking, particularly when compared to plane wave optics. In this work we are particularly interested in the optical helicity and SAM of non-paraxial electromagnetic fields generated by tightly focusing optical vortices. Optical helicity is the property of light responsible for non-mechanical chiral light-matter interactions and optical activity[6,7]; SAM is responsible for the mechanical spinning of probe particles. One of the remarkable properties of non-paraxial fields is that they generate a transverse (with respect to the direction of propagation) SAM density[8–12].

In contrast to propagating plane waves and paraxial fields which possess optical helicity proportional to the degree of circular polarization, here we highlight that tightly focused optical vortices possess a non-zero optical helicity density for both a linearly polarized input beam and even more remarkably an *unpolarized* input beam (i.e. both have zero degree of circular polarization). Furthermore, we also highlight how a tightly focused linearly polarized optical vortex generates a longitudinal SAM density. Whilst many novel effects of non-paraxial fields compared to paraxial fields are now known (e.g. transverse spin), the key thing to note is that the phenomena highlighted in this work are unique to non-paraxial optical vortices, even when compared to other non-paraxial optical fields.

Complex Light and Optical Forces XVI, edited by David L. Andrews, Enrique J. Galvez, Halina Rubinsztein-Dunlop, Proc. of SPIE Vol. 12017, 1201708
 · 0277-786X · doi: 10.1117/12.2605929

2. 3D LAGUERRE-GAUSSIAN MODES

We refer to light as being 2D structured if it is inhomogeneous in the transverse plane (x,y) but is homogenous along the direction of propagation (z)[13]. Examples of 2D structured optical fields would be paraxial optical vortices (phase structured) or vector beams (polarization structured)[14]. 3D structured light manifests when an optical field is spatially confined, examples include evanescent waves or tightly focussed laser beams. The key physical property of 3D structured light, that which is responsible for much of their extraordinary properties, is the fact it exhibits longitudinal (with respect to the direction of propagation) electromagnetic field components. The magnitude of longitudinal fields is proportional to a smallness parameter, in the case of focused laser beams for example it is $\left(\lambda / 2\pi w_0\right)^{-1}$, and under very tight focusing they can exceed transverse field components. The quantum electrodynamical (QED) electric $\boldsymbol{e}^{\perp}\left(\boldsymbol{r}\right)$ (the superscript denotes transversality with respect to the Poynting vector) and magnetic mode $\boldsymbol{b}\left(\boldsymbol{r}\right)$ expansions for a circularly polarized source which include the first-order longitudinal field components are[15]

$$\boldsymbol{e}^{\perp}\left(\boldsymbol{r}\right) = i\sum_{k,\sigma,\ell,p}\left(\frac{\hbar ck}{2\varepsilon_0 A_{\ell,p}^2 V}\right)^{1/2}\frac{1}{\sqrt{2}}\left[\left\{\left(\hat{\boldsymbol{x}}+i\sigma\hat{\boldsymbol{y}}\right)+\frac{i}{k}\hat{\boldsymbol{z}}\left(\frac{\partial}{\partial r}-\ell\sigma\frac{1}{r}\right)\mathrm{e}^{i\sigma\phi}\right\}\right.$$
$$\left.\times f_{|\ell|,p}\left(r\right)a_{|\ell|,p}{}^{(\sigma)}\left(k\hat{\boldsymbol{z}}\right)\mathrm{e}^{i(kz+\ell\phi)}-\mathrm{H.c}\right], \tag{1}$$

and

$$\boldsymbol{b}\left(\boldsymbol{r}\right) = i\sum_{k,\sigma,\ell,p}\left(\frac{\hbar k}{2c\varepsilon_0 A_{\ell,p}^2 V}\right)^{1/2}\frac{1}{\sqrt{2}}\left[\left\{\left(\hat{\boldsymbol{y}}-i\sigma\hat{\boldsymbol{x}}\right)+\frac{1}{k}\hat{\boldsymbol{z}}\left(\sigma\frac{\partial}{\partial r}-\frac{\ell}{r}\right)\mathrm{e}^{i\sigma\phi}\right\}\right.$$
$$\left.\times f_{|\ell|,p}\left(r\right)a_{|\ell|,p}{}^{(\sigma)}\left(k\hat{\boldsymbol{z}}\right)\mathrm{e}^{\,i(kz+\ell\phi)}-\mathrm{H.c}\right]. \tag{2}$$

where $k=2\pi/\lambda$ is the wavenumber, V is a quantization volume, $A_{\ell,p}^2$ is a normalization constant for LG modes, $\sigma=\pm1$, the positive sign designates left-handed CPL; the negative sign right-handed CPL, $a_{|\ell|,p}{}^{(\sigma)}\left(k\hat{\boldsymbol{z}}\right)$ is the annihilation operator, $\exp i\left(kz+\ell\phi\right)$ is the phase, $\ell\in\mathbb{Z}$ is the topological charge, H.c. stands for Hermitian conjugate, and $f_{|\ell|,p}\left(r\right)$ is the radial distribution function around the focal plane

$$f_{|\ell|,p}\left(r\right) = \frac{C_p^{|\ell|}}{w_0}\left(\frac{\sqrt{2}r}{w_0}\right)^{|\ell|}\mathrm{e}^{-\frac{r^2}{w_0^2}}L_p^{|\ell|}\left[\frac{2r^2}{w_0^2}\right], \tag{3}$$

where w_0 is the beam waist, the normalization constant is given by $C_p^{|\ell|} = \sqrt{2p!/\left[\pi\left(p+|\ell|\right)!\right]}$ and $L_p^{|\ell|}$ is the generalised Laguerre polynomial of order *p*.

3. OPTICAL HELICITY AND CHIRALITY DENSITY

For the monochromatic fields used throughout this work, the optical helicity $\mathcal{H}$ and optical chirality X are directly proportional $\mathcal{H} = X/ck^2$ [16]. The optical helicity in QED is given as[17]

$$\mathcal{H} = \varepsilon_0 c \int d^3\boldsymbol{r}\left(-\int \boldsymbol{e}^{\perp} dt\right)\cdot \boldsymbol{b}. \tag{4}$$

For the remainder of this work we are interested in the integrand of (4), the optical helicity density h, along with the understanding it is directly proportional to the optical chirality density χ. For an input laser mode (k,σ,ℓ,p) of n photons $\left|n(k,\sigma,\ell,p)\right\rangle$, using (1) and (2) in (4) we produce the following optical helicity density for a 2D-circularly polarized 3D LG mode (2D-circularly polarized means the transverse field is circularly polarized):

$$h = \sum_{\sigma,\ell,p}\left(\frac{n\hbar}{A_{\ell,p}^2 V}\right)\left[\sigma f^2 + \frac{1}{2k^2}\left(\sigma f'^2 - \frac{2\ell}{r} ff' + \frac{\ell^2\sigma}{r^2} f^2\right)\right]. \tag{5}$$

We have dropped the dependencies of the factors for notational brevity (the prime denotes partial differentiation with respect to *r*). Setting $\ell = 0$ in (5) gives us the helicity density of a fundamental Gaussian beam, dependent solely on the sign of σ (alternatively put, the handedness of the input circular polarization). More interesting physics manifests for tightly focused ($w_0 = \lambda$ in all simulations) LG modes where $\ell \neq 0$. First we have the potential for an interplay between angular momentum via the two distinct combinations of parallel $\operatorname{sgn}\sigma = \operatorname{sgn}\ell$ or anti-parallel $\operatorname{sgn}\sigma = -\operatorname{sgn}\ell$ combinations of SAM and OAM, as highlighted in Figure 1.

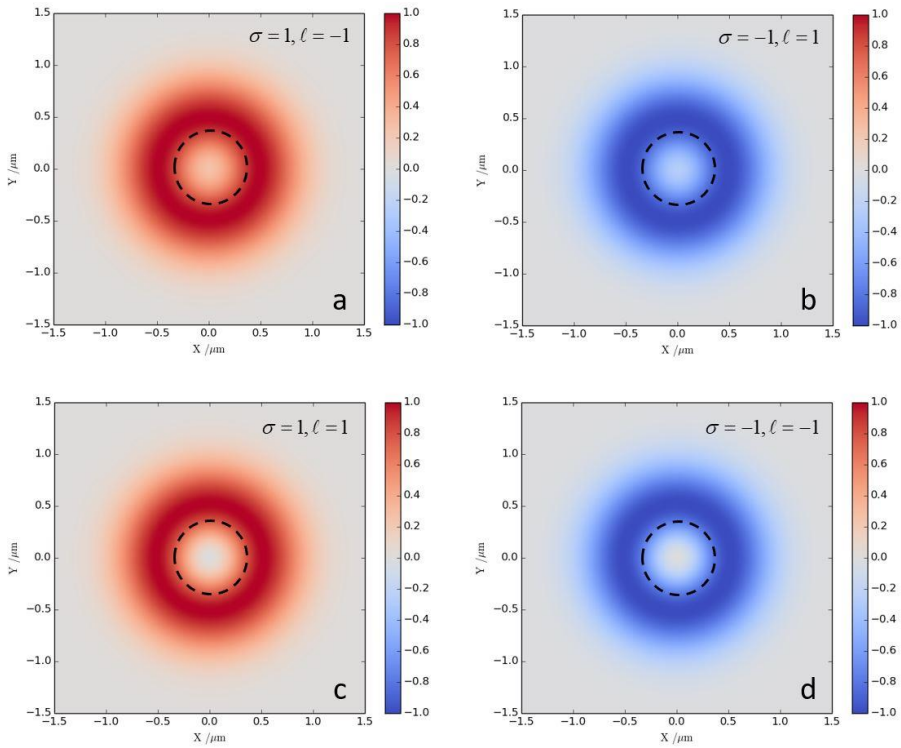

Figure 1: normalised optical helicity (chirality) density distribution equation (5) in the focal plane for $w_0 = \lambda$ a) $\sigma = 1, \ell = -1$ b) $\sigma = -1, \ell = 1$ c) $\sigma = 1, \ell = 1$ d) $\sigma = -1, \ell = -1$. $p = 0$ (a)-(d). The helicity densities in a) and b) have a major contribution from the zeroth-order transverse fields which is $\propto r^2$ and a smaller, on-axis contribution from the longitudinal fields (i.e. $\propto r^0$); the helicity densities in c) and d) have a major contribution from zeroth-order transverse fields that is $\propto r^2$, but the longitudinal contributions in this case are $\propto r^4$. Dashed circles aid visual clarity of the non-zero on-axis helicity density in the cases where $\operatorname{sgn}\sigma = -\operatorname{sgn}\ell$.

Significantly more interesting however is that setting $\sigma = 0$ gives a non-zero helicity density for a 2D-linearly polarized 3D LG beam:

$$h = -\sum_{\ell,p}\left(\frac{n\hbar}{A_{\ell,p}^2 V}\right)\frac{\ell}{k^2 r} ff'. \tag{6}$$

The helicity density (6) is plotted in Figure 2 for $\ell = \pm 1, \pm 2; p = 0$. It has recently been shown that the optical helicity density (6) produces discriminatory radial forces on a mixture of chiral particles, enabling the separation of right- and left-handed enantiomers into distinct rings in the transverse plane[18] (See Fig 2.).

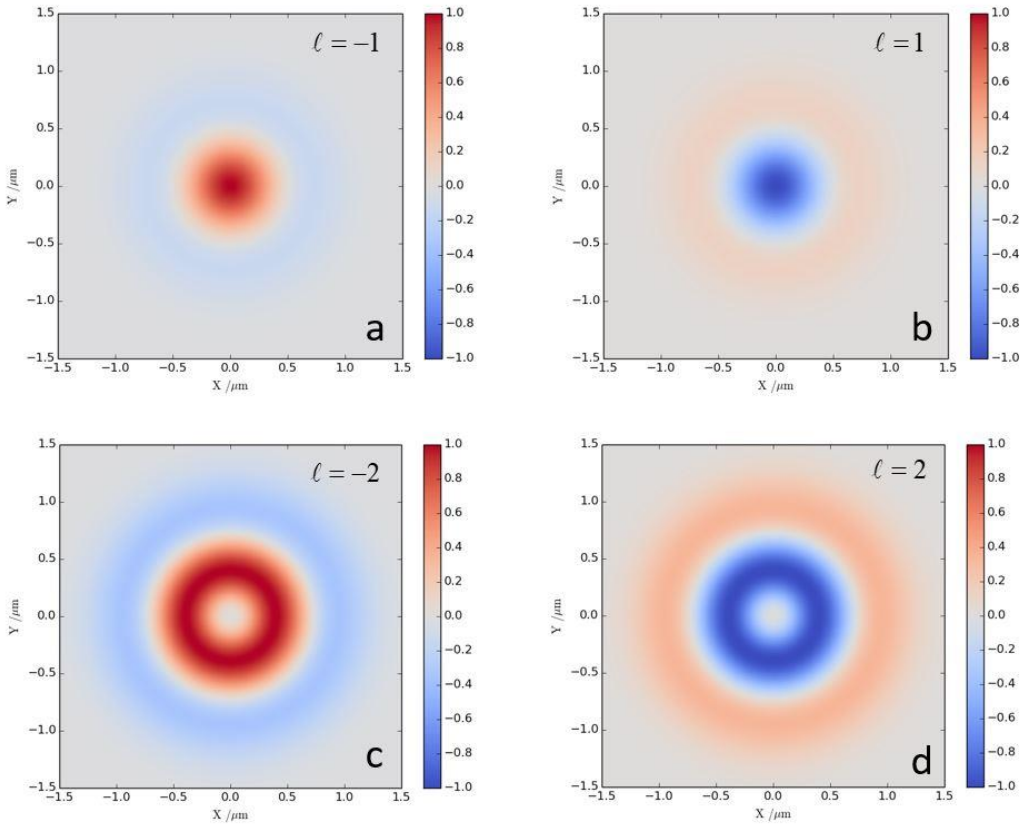

Figure 2: normalized polarization-independent optical helicity density (6) at $w_0\left(z=0\right)$. $p=0$ in (a)-(d).

This remarkable result was first theorized for a coherent superposition of Bessel beams by Rosales-Guzmán et al.[19] and later observed experimentally for a tightly focused 2D-linearly polarized LG beam by Banzer's group[20]. It is important to note that the integrated value of (6), i.e. $\mathcal{H}$, is zero and so probe particles must be smaller than the transverse width of beam[21]. The story does not end here, however, and it has recently been highlighted[22] that a 2D-unpolarized vortex beam can generate a non-zero optical helicity density when tightly-focused, which is in stark contrast to the prevailing textbook understanding of light's optical chirality and helicity. Though an extraordinary result, it is relatively easy to show. In order to get the observable optical helicity density for a 2D-unpolarized input beam we need to average the result over two orthogonal polarizations on the Poincare sphere. Right- and left-handed circular polarized beams are orthogonal, and so averaging the two results of (5) when $\sigma=1$ and $\sigma=-1$ we yield

$$h^n=\frac{h^{|\sigma|}+h^{-|\sigma|}}{2}=-\sum_{\ell,p}\left(\frac{n\hbar}{A_{\ell,p}^2V}\right)\frac{\ell}{k^2r}\,ff', \tag{7}$$

which is identical to (6) and so the optical helicity density spatial distributions of a tightly focused 2D-unpolarized optical vortex are the same as those given in Figure 2. Because (7) is directly proportional to ℓ, a fundamental Gaussian beam does not possess an optical helicity density for an unpolarized mode, nor does an evanescent wave. Interestingly, however,

the latter two optical fields do possess a non-zero transverse spin momentum density when generated from a 2D-unpolarized source[23]. The distinguishing feature between optical vortex modes and non-vortex paraxial modes/ evanescent waves is that the former possess the azimuthal phase $\exp(i\ell\phi)$ which yields an azimuthal component of the canonical momentum density, and when projected on to a transverse spin density gives a non-zero optical helicity, i.e. (5)-(7). The non-vortex optical fields possess a canonical momentum density in the direction of propagation only, which projected on to transverse spin momentum generated by linearly polarized or unpolarized optical fields (neccesarily with zero longitudinal spin) clearly gives zero.

4. SPIN ANGULAR MOMENTUM

The SAM density is given in QED as[17]

$$\boldsymbol{s} = \frac{\varepsilon_0}{2}\left(-\boldsymbol{e}^{\perp}\times\int \boldsymbol{e}^{\perp}dt - \frac{1}{c}\boldsymbol{b}\times\int \boldsymbol{b}dt\right). \tag{8}$$

The (longitudinal) SAM density which stems purely from the dominant zeroth-order transverse fields is well known to be proportional to the degree of circular polarization. Linearly polarized/unpolarized plane waves and paraxial fields have zero SAM. The extraordinary transverse spin momentum[9–12] density stems from the cross product of the zeroth-order transverse field and the first-order longitudinal field. For a 2D-linearly polarized 3D LG mode it is:

$$\begin{aligned}\boldsymbol{s}_{\perp} &= \sum_{k,\ell,p}\left(\frac{n\hbar}{A_{\ell,p}^2 V}\right)\left[\underbrace{\hat{\boldsymbol{x}}\frac{1}{k}(\sin\phi)\frac{\partial}{\partial r}}_{s_x^b} - \underbrace{\hat{\boldsymbol{y}}\frac{1}{k}(\cos\phi)\frac{\partial}{\partial r}}_{s_y^e}\right] ff \\ &= -\hat{\boldsymbol{\phi}}\sum_{k,\ell,p}\left(\frac{n\hbar}{A_{\ell,p}^2 V}\right)\frac{1}{k}\, ff',\end{aligned} \tag{9}$$

where $\boldsymbol{s}_x^b$ is the magnetic field contribution and $\boldsymbol{s}_y^e$ is the electric field contribution. The individual $\boldsymbol{s}_x^b$ and $\boldsymbol{s}_y^e$, as well as the total $\boldsymbol{s}_{\phi}^{e+b}$, parts of (9) are plotted in Figure 8 for $\ell = 1, p = 0, w_0 = \lambda$.

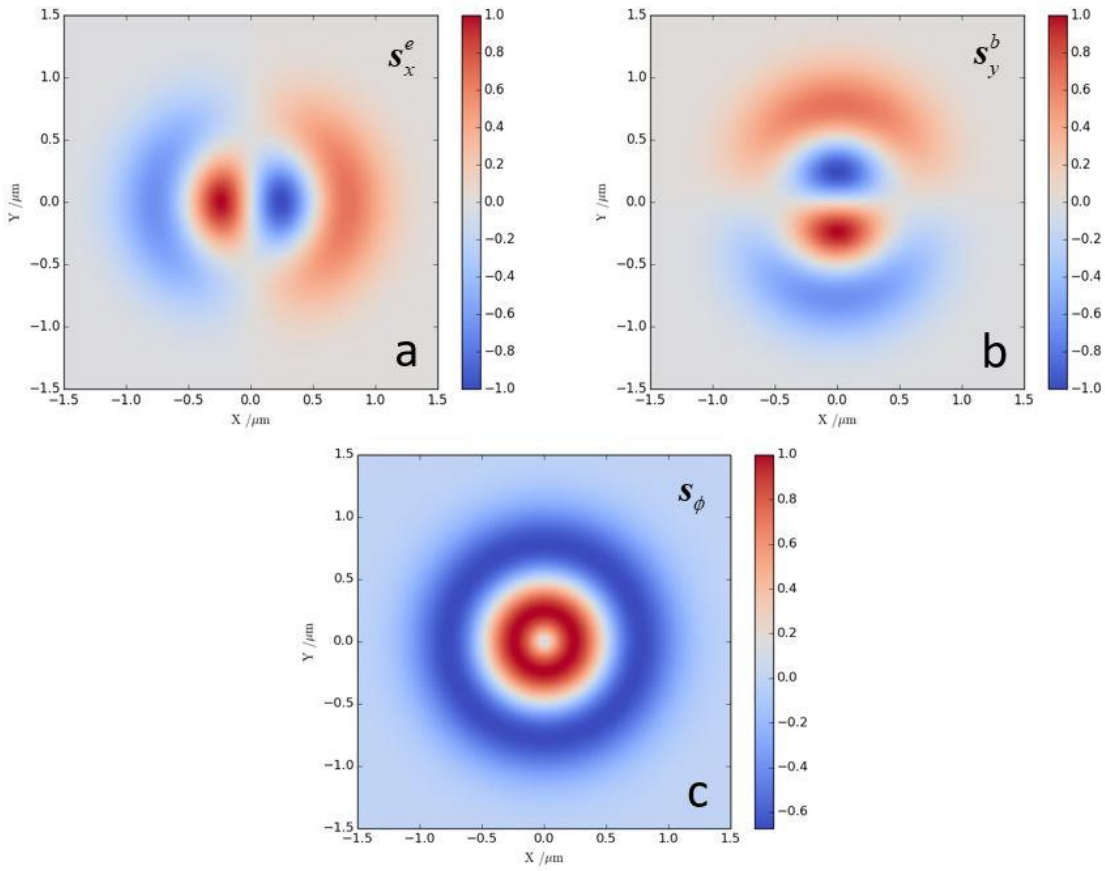

Figure 3: Components of transverse SAM density (a) s_y^e term in equation (9) ; (b) s_x^b term in equation (9); and (c) the total s_ϕ^{e+b} Eq. (9). $|\ell| = 1, p = 0, w_0 = \lambda$ for (a)-(c).

Just as it was shown in the previous section that 3D optical vortices possess a unique optical helicity density for 2D-unpolarized inputs (unique even compared to other non-paraxial optical fields), they also uniquely possess a SAM density in the direction of propagation for 2D-linearly polarized inputs. This contribution stems from the cross product of the zeroth-order transverse field and the second-order transverse fields. This longitudinal spin for linearly polarized tightly focused optical vortices is given as (complete calculations can be found in Ref[17])

$$\begin{aligned} \boldsymbol{s}_{\parallel} &= \sum_{k,\ell,p}\left(\frac{n\hbar}{A_{\ell,p}^2 V}\right)\frac{2}{k^2}\hat{\boldsymbol{z}}\Bigg[\underbrace{\left\{\cos^2\phi\left(\frac{\partial}{\partial r}\frac{\ell}{r}\right)+\frac{\ell}{r^2}\sin^2\phi-\frac{\ell}{r}\frac{\partial}{\partial r}\sin^2\phi\right\}}_{s_z^e} \\ &+\underbrace{\left\{\sin^2\phi\left(\frac{\partial}{\partial r}\frac{\ell}{r}\right)+\frac{\ell}{r^2}\cos^2\phi-\frac{\ell}{r}\frac{\partial}{\partial r}\cos^2\phi\right\}}_{s_z^b}\Bigg] ff \\ &= \sum_{k,\ell,p}\left(\frac{n\hbar}{A_{\ell,p}^2 V}\right)\frac{2}{k^2}\hat{\boldsymbol{z}}\left[\left(\frac{\partial}{\partial r}\frac{\ell}{r}\right)+\frac{\ell}{r^2}-\frac{\ell}{r}\frac{\partial}{\partial r}\right] ff. \end{aligned} \tag{10}$$

Remarkably what this shows is that there exists a SAM density in the direction of propagation even for 2D-linearly polarized 3D optical vortices[24–26]. Note that each term in (10) is dependent on ℓ and so this phenomenon is unique to optical vortices: a linearly polarised Gaussian beam $\ell = 0$ does not possess this longitudinal SAM density. The total dual symmetric contribution (10) is actually zero due to (again, see Ref[17] for further details).

$$f\frac{\partial}{\partial r}\frac{\ell}{r}f = -\frac{\ell}{r^2}f^2 + \frac{\ell}{r}ff'. \tag{11}$$

Experimentally of course light-matter interactions are generally dominated by electric dipole coupling and so the electric field contribution to (10) should be observable provided kw_0 is small enough. The individual electric $\boldsymbol{s}_z^e$ and magnetic $\boldsymbol{s}_z^b$ contributions of Eq. (10) are plotted in Fig. 4. Unlike the optical helicity density which persists for 2D-unpolarized 3D LG beams in the previous section, a 2D-unpolarized 3D vortex beam possesses zero longitudinal spin (10).

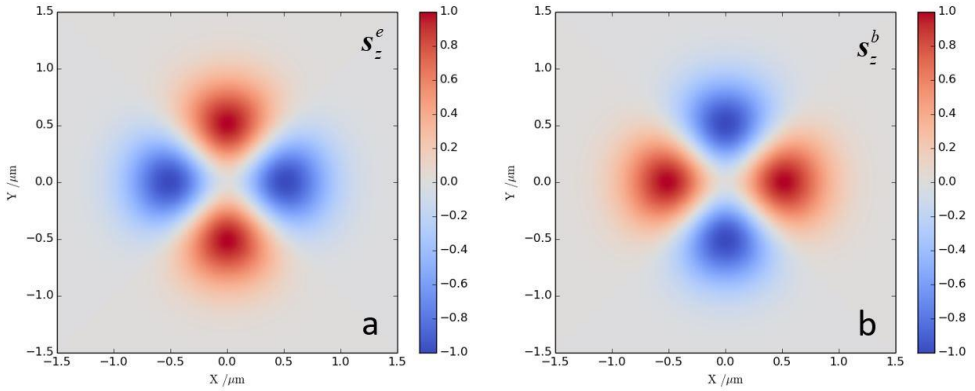

Figure 4: Components of longitudinal SAM density of (a) $\boldsymbol{s}_z^e$ term in equation (10); (b) $\boldsymbol{s}_z^b$ term in Eq. (10) $|\ell| = 1, p = 0, w_0 = \lambda$ for (a)-(b).

5. CONCLUSION

Non-paraxial optical fields offer a plethora of novel physics and applications in nanophotonics compared to plane wave and paraxial optics. Using a QED formulation, we have highlighted two novel properties of non-paraxial optical vortices: 1) a non-zero optical helicity (chirality) density for 2D-unpolarised (and 2D-linearly polarized) 3D optical vortices and 2) a longitudinal spin angular momentum density for 2D-linearly polarized 3D optical vortices. The key result is that both results are unique to non-paraxial optical vortices, even when compared to other non-paraxial optical fields such as tightly focused non-vortex laser beams and evanescent waves. This work adds to the rapidly growing field of optical vortices and chirality[27] and optical nanomanipulation with structured light[28].

ACKNOWLEDGEMENTS

KAF thanks the Leverhulme Trust for funding him through a Leverhulme Early Career Fellowship ECF-2019-398.

REFERENCES

1. Bliokh, K. Y., Bekshaev, A. Y. & Nori, F. Dual electromagnetism: helicity, spin, momentum and angular momentum. *New J. Phys.* **15**, 033026 (2013).
2. Born, M. & Wolf, E. *Principles of optics: electromagnetic theory of propagation, interference and diffraction of light*. (Elsevier, 2013).
3. Zangwill, A. *Modern electrodynamics*. (Cambridge University Press, 2013).
4. Hecht, E. *Optics*. (Pearson Education, 2015).
5. Novotny, L. & Hecht, B. *Principles of Nano-Optics*. (Cambridge University Press, 2012).
6. Cameron, R. P., Barnett, S. M. & Yao, A. M. Optical helicity, optical spin and related quantities in electromagnetic theory. *New J. Phys.* **14**, 053050 (2012).
7. Crimin, F., Mackinnon, N., Götte, J. B. & Barnett, S. M. Optical helicity and chirality: conservation and sources. *Appl. Sci.* **9**, 828 (2019).
8. Bliokh, K. Y., Bekshaev, A. Y. & Nori, F. Extraordinary momentum and spin in evanescent waves. *Nat. Commun.* **5**, 3300 (2014).
9. Aiello, A., Banzer, P., Neugebauer, M. & Leuchs, G. From transverse angular momentum to photonic wheels. *Nat. Photonics* **9**, 789–795 (2015).
10. Neugebauer, M., Bauer, T., Aiello, A. & Banzer, P. Measuring the transverse spin density of light. *Phys. Rev. Lett.* **114**, 063901 (2015).
11. Neugebauer, M., Eismann, J. S., Bauer, T. & Banzer, P. Magnetic and Electric Transverse Spin Density of Spatially Confined Light. *Phys. Rev. X* **8**, 021042 (2018).
12. Bliokh, K. Y. & Nori, F. Transverse and longitudinal angular momenta of light. *Phys. Rep.* **592**, 1–38 (2015).
13. Forbes, A., de Oliveira, M. & Dennis, M. R. Structured light. *Nat. Photonics* **15**, 253–262 (2021).
14. Angelsky, O. V. *et al.* Structured Light: Ideas and Concepts. *Front. Phys.* **8**, (2020).

15. Forbes, K. A., Green, D. & Jones, G. A. Relevance of longitudinal fields of paraxial optical vortices. *J. Opt.* **23**, 075401 (2021).
16. Mackinnon, N. On the differences between helicity and chirality. *J. Opt.* **21**, 125402 (2019).
17. Forbes, K. A. & Jones, G. A. Measures of helicity and chirality of optical vortex beams. *J. Opt.* **23**, 115401 (2021).
18. Forbes, K. A. & Green, D. Enantioselective optical gradient forces using 3D structured vortex light. *ArXiv211212470 Phys.* (2021).
19. Rosales-Guzmán, C., Volke-Sepulveda, K. & Torres, J. P. Light with enhanced optical chirality. *Opt. Lett.* **37**, 3486–3488 (2012).
20. Woźniak, P., Leon, I. D., Höflich, K., Leuchs, G. & Banzer, P. Interaction of light carrying orbital angular momentum with a chiral dipolar scatterer. *Optica* **6**, 961–965 (2019).
21. Forbes, K. A. & Jones, G. A. Optical vortex dichroism in chiral particles. *Phys. Rev. A* **103**, 053515 (2021).
22. Forbes, K. A. Optical helicity of unpolarized light. *ArXiv211211555 Phys.* (2021).
23. Eismann, J. S. *et al.* Transverse spinning of unpolarized light. *Nat. Photonics* **15**, 156–161 (2021).
24. Li, M. *et al.* Orbit-induced localized spin angular momentum in strong focusing of optical vectorial vortex beams. *Phys. Rev. A* **97**, 053842 (2018).
25. Yu, P., Zhao, Q., Hu, X., Li, Y. & Gong, L. Orbit-induced localized spin angular momentum in the tight focusing of linearly polarized vortex beams. *Opt. Lett.* **43**, 5677–5680 (2018).
26. Hang, L., Wang, Y. & Chen, P. Symmetry of electric spin angular momentum density in the tight focusing of linearly polarized vortex beams. *J. Opt. Soc. Am. A* **36**, 1374 (2019).
27. Forbes, K. A. & Andrews, D. L. Orbital angular momentum of twisted light: chirality and optical activity. *J. Phys. Photonics* **3**, 022007 (2021).
28. Yang, Y., Ren, Y., Chen, M., Arita, Y. & Rosales-Guzmán, C. Optical trapping with structured light: a review. *Adv. Photonics* **3**, 034001 (2021).